

Received February 8, 2022, accepted February 25, 2022, date of publication March 2, 2022, date of current version March 10, 2022.

Digital Object Identifier 10.1109/ACCESS.2022.3156080

Underground Target Localization Based on Improved Magnetic Gradient Tensor With Towed Transient Electromagnetic Sensor Array

LIJIE WANG¹, SHUANG ZHANG¹, SHUDONG CHEN¹, AND CHAOPENG LUO²

¹College of Electronic Science and Engineering, Jilin University, Changchun 130012, China

²Science and Technology on Near-Surface Detection Laboratory, Wuxi 214035, China

Corresponding authors: Shudong Chen (chenshudong@jlu.edu.cn) and Chaopeng Luo (harbour122254744@gmail.com)

This work was supported in part by the Science and Technology on Near Surface Detection Laboratory under Grant TCGZ2017A003, Grant TCGZ2018A009, and Grant 6142414190906; and in part by the National Natural Science Foundation of China under Grant 41704145.

ABSTRACT Errors of target localization with the traditional magnetic gradient tensor mainly comes from three aspects, namely, the large error of the magnetic gradient tensor for shallow targets, the low signal-to-noise ratio (SNR) of the response for deep targets, and the overlapping responses of multi-targets. In this study, a towed transient electromagnetic sensor with a 3×3 receiving coils array is constructed. On the basis of the sensor array, an improved magnetic gradient tensor is proposed to accurately locate targets. For shallow targets, the magnetic gradient tensor is constructed using the responses of four adjacent receiving coils to reduce the error of the magnetic gradient tensor. For deep targets, all the responses of nine receiving coils are used to improve the SNR. Both the early and late time responses are used to roughly estimate the positions of multi-targets to improve the localization accuracy. Experimental results show that for underground targets within 2 m, the depth errors of the targets do not exceed 10 cm, and the horizontal errors of the targets are mostly within 10 cm, even if the responses of two adjacent targets overlap each other, indicating that the proposed method can effectively improve the localization accuracy of underground targets.

INDEX TERMS Towed transient electromagnetic sensor array, unexploded ordnance (UXO), target localization, magnetic gradient tensor.


I. INTRODUCTION

Unexploded ordnances (UXO) seriously threaten human security and hinder economic construction and land reuse [1]. Many harmless targets, such as metal fragments and shrapnel, are usually scattered around UXOs, resulting in a high false alarm rate of detection [2]. Therefore, the quick and accurate detection and identification of UXOs from these harmless targets have become a concern of researchers at home and abroad [3].

In recent years, different kinds of UXO detection methods, such as ground-penetrating radar (GPR) [4], [5], magnetic detection [6], [7], electromagnetic induction (EMI) [8], [9], infrared detection, and microgravity detection, have been widely developed and applied with the development of detection technology. GPR can locate underground targets by transmitting high-frequency electromagnetic waves, which

are easily affected by geological conditions. Magnetic detection has high efficiency and low cost but can only detect magnetic targets. The working frequency of EMI ranges from tens to hundreds of kHz, including frequency and time domain detections. EMI can detect magnetic and non-magnetic targets with a strong anti-interference ability. Transient electromagnetic (TEM) detection has been effectively used for underground target detection.

The clearance of UXO is mainly achieved in three steps: detection, inversion, and identification. In the detection step, various TEM systems are designed and developed based on different detection platforms to locate underground targets. Portable and vehicle systems are two typical detection systems. These TEM systems usually include two working modes: the survey and cued modes. The position of underground targets can be roughly determined according to the maximum response in the survey mode. The target position can be accurately calculated by different algorithms according to the measured response in the cued mode.

The associate editor coordinating the review of this manuscript and approving it for publication was Kai-Da Xu .

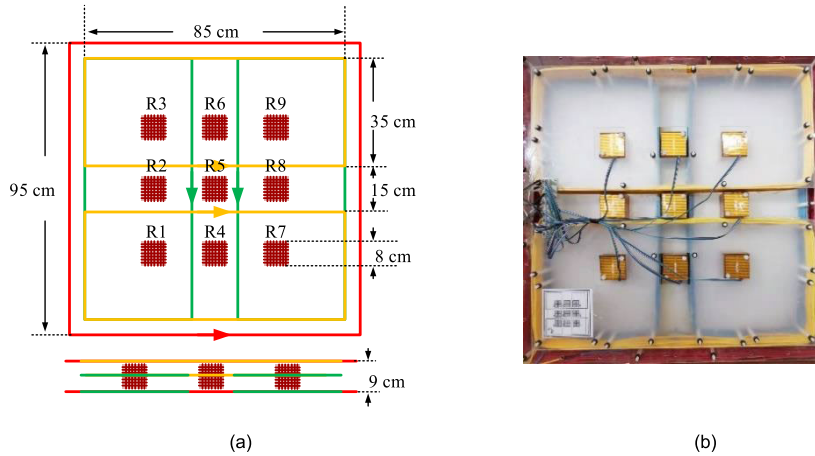


FIGURE 1. (a) Structure of the towed array system, (b) picture of the system.

TABLE 1. Parameters of the towed system.

Coil		Length (cm)	Number of turns	Resistance (Ω)	Inductance (mH)
Transmitting coils	x	35×85	20	0.556	1.312
	y	35×85	20	0.564	1.316
	z	95×95	20	0.468	0.958
Receiving coils		8	480	112	19

Portable systems, like the MPV-I, MPV-II systems designed by G & G Sciences [10], [11], and the portable metal detector designed by Jilin University [12], have effectively detected underground targets. Vehicle systems, like Metal-Mapper [13], Berkeley UXO Discriminator [14], and the Time-domain Electromagnetic Multi-sensor Tower Array Detection System, were developed to detect underground targets [15]. Compared with portable systems, these vehicle systems usually adopt large transmitting magnetic moments, multiple transmitters, and multiple receivers to detect deep and large area targets.

A magnetic gradient tensor can locate a single target without iteration and has been effectively used in magnetic detection [16]. The localization accuracy of a magnetic gradient tensor is related to the sensor signal-to-noise ratio (SNR) and the target depth. In TEM detection, the target localization error of the magnetic gradient tensor is large due to the influence of the overlapping response of adjacent targets. In this paper, the combination of the magnetic gradient tensor with the early and late responses of the target is proposed to improve the localization accuracy of overlapping signals. First, the target position is roughly estimated based on the towed TEM system. And, the number of underground targets is preliminarily determined with the maxima of the early and late responses. Then, the target position can be further estimated accurately with the constructed magnetic gradient tensors.

The rest of this paper is organized as follows. Section II mainly introduces the towed TEM system and the single

dipole model. Section III provides a detailed introduction to magnetic gradient tensor localization. Section IV presents the experimental results and discussion. Section V presents the conclusions.

II. BASIC METHOD

Target responses are obtained by the towed TEM array system, and data processing is based on the single dipole model.

A. TOWED TEM SYSTEM

The towed TEM system consists of three transmitting coils (i.e., the x, y, and z components) and nine three-component receiving coils, which operate in two modes. In the survey mode, the z component transmitting coil transmits the current in the frequency of 125 Hz to roughly estimate the location of underground targets. In the cued mode, three transmitting coils sequentially emit currents with a frequency of 12.5 Hz to excite the underground target. The 3 × 3 array receiving coils synchronously collect responses. The structure and picture of the system are shown in Figure 1.

As shown in Figure 1(a), the green, yellow, and red squares are the respective x, y, and z component transmitting coils wound by overlapping loops with a copper line with a cross-area of 6 mm². The x and y component transmitting coils are constructed with two inverted series rectangular coils. The 9 three-component receiving coils are designed in a 3 × 3 array with a 20-cm interval. The side length, the resonance frequency, and the distance between the sections of each receiving coil are 8 cm, 230 kHz, and 7 mm, respectively. The nine receiving coils adopt the combination of double-layer shielding and center tapped grounding to improve the SNR of the receiving response. Figure 1(b) is physical picture of the system. Table 1 presents the parameters.

On the basis of the sensor design above, this study completed the target localization according to the single dipole model.

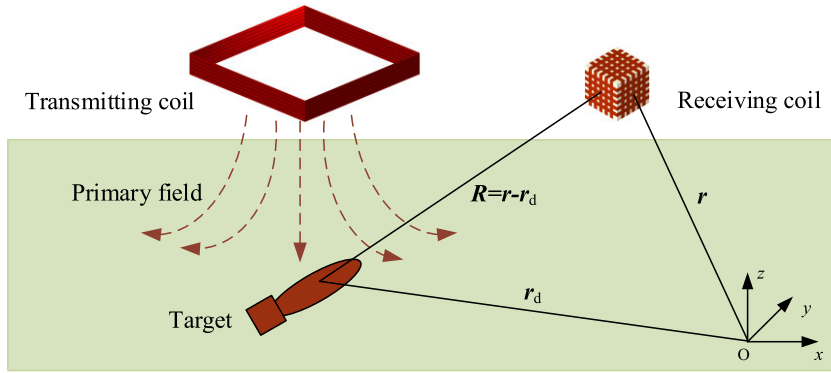


FIGURE 2. Principle of the target detection based on the dipole model.

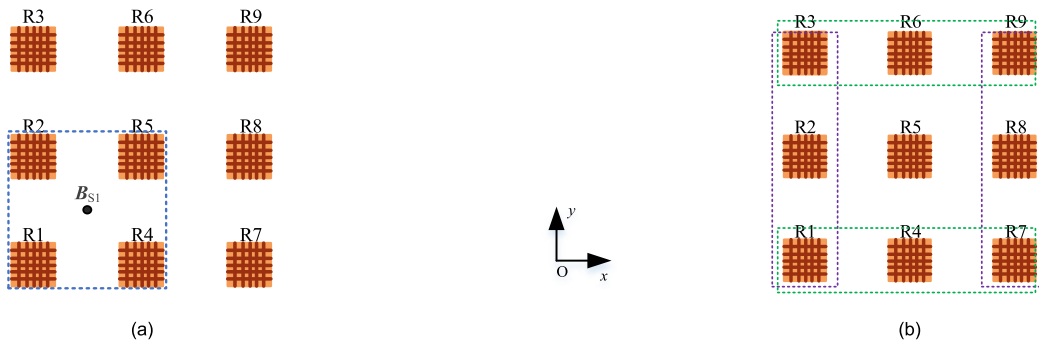


FIGURE 3. (a) Target localization with 4 coils, (b) target localization with 9 coils.

B. SINGLE DIPOLE MODEL

When the distance between the sensor and an underground target is more than 2.5 times the target size, the target can usually be treated as a dipole model for data processing [17].

As shown in Figure 2, the secondary field (B_S) of the underground target at the position (r) of the receiving coil can be denoted as

$$B_S = \frac{1}{4\pi R^3} (3e'_R e_R - I)m = G(R)m, \quad (1)$$

where $e_R = \mathbf{R}/|\mathbf{R}|$, $|\mathbf{R}|$ is the modulus of position $\mathbf{R} = \mathbf{r} - \mathbf{r}_d$. \mathbf{r}_d represents the target position. The size of identity matrix I is 3×3 . $G(\mathbf{R})$ is Green's function, which only depends on target position \mathbf{R} . Dipole moment \mathbf{m} is expressed as

$$\mathbf{m} = \mathbf{M}\mathbf{B}_p(\mathbf{r}_d), \quad (2)$$

where \mathbf{M} is the magnetic polarizability tensor, which is a symmetric matrix and is determined by the shape, size, orientation, permeability, and conductivity of the target. \mathbf{B}_p represents the primary field of the target.

III. TARGET LOCALIZATION

A. MAGNETIC GRADIENT TENSOR

The target position can be effectively estimated by the magnetic gradient tensor in magnetic detection. According to Equation (1), the difference between the secondary field (B_S')

at position $\mathbf{R} + \mathbf{n} d\mathbf{R}$ and the B_S at position \mathbf{R} is expressed as [18]

$$\begin{aligned} B_S' - B_S &= \frac{\mu}{4\pi} [3(\mathbf{m} \cdot \mathbf{e}_R)\mathbf{e}_R - \mathbf{m}] \left(\frac{\partial}{\partial R} \frac{1}{R^3} d\mathbf{R} \right) \\ &= -\frac{3}{R} \mathbf{B}_S d\mathbf{R}, \end{aligned} \quad (3)$$

which can be rewritten as

$$\mathbf{G}\mathbf{R} = -3\mathbf{B}_S, \quad (4)$$

where \mathbf{G} is the magnetic gradient tensor, which is a symmetric matrix and expressed as

$$\mathbf{G} = \begin{bmatrix} \partial B_x / \partial x & \partial B_x / \partial y & \partial B_x / \partial z \\ \partial B_y / \partial x & \partial B_y / \partial y & \partial B_y / \partial z \\ \partial B_z / \partial x & \partial B_z / \partial y & \partial B_z / \partial z \end{bmatrix}. \quad (5)$$

According to Equation (4), target position \mathbf{R} is denoted as

$$\mathbf{R} = -3\mathbf{G}^{-1}\mathbf{B}_S. \quad (6)$$

The sum of the diagonal elements for \mathbf{G} is zero. Five independent elements of matrix \mathbf{G} must be calculated.

For shallow targets, that is, the target depth is near the distance between the two receiving coils, a large error of the magnetic gradient is obtained. The error will decrease as the target depth increases. For different target depths, two

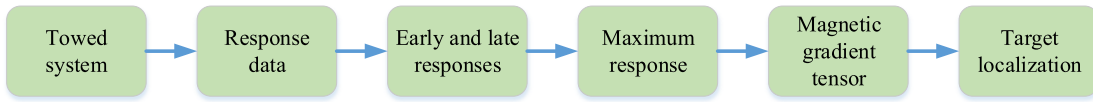


FIGURE 4. Process of target localization.

TABLE 2. Parameters of targets.

UXOs	Name	U1	U2	U3	U4	U5	U6	U7	U8	U9	U10	U11	U12
	Length (cm)	18	26	24	27	34	35	39	51	46	55	58	65
	Diameter (mm)	37	57	60	82	75	74	85	100	100	122	120	130
Harmless targets	Name	O1	O2	O3	O4	O5	O6	O7	O8	O9			
	Length (cm)	16	25	5	10	20	30	2	/	12.5			
	Diameter (mm)	30	37	75	75	75	75	150	64	/			

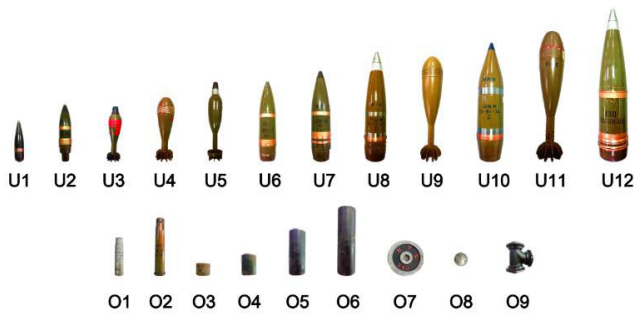


FIGURE 5. Diagram of the targets.

magnetic gradient tensor algorithms are proposed to improve the localization accuracy.

The magnetic gradient tensor constructed in Figure 3(a) is used to locate shallow targets, and that in Figure 3(b) is used to locate deep targets. In Figure 3(a), B_{S1} is the equivalent central response of the four coils (R1, R4, R2, and R5), which is expressed as

$$B_{S1} = \frac{B_1 + B_2 + B_4 + B_5}{4}, \quad (7)$$

where $B_1, B_2, B_4,$ and B_5 are the target responses acquired by receiving coils R1, R2, R4, and R5, respectively. According to the four receiving coils in Figure 3(a), the five independent elements of matrix G are expressed as follows:

$$\begin{cases} \partial B_x / \partial x = (B_{4x} + B_{5x} - B_{1x} - B_{2x}) / 2d \\ \partial B_x / \partial y = (B_{4y} + B_{5y} - B_{1y} - B_{2y}) / 2d \\ \partial B_x / \partial z = (B_{4z} + B_{5z} - B_{1z} - B_{2z}) / 2d \\ \partial B_y / \partial y = (B_{2y} + B_{5y} - B_{1y} - B_{4y}) / 2d, \\ \partial B_y / \partial z = (B_{2z} + B_{5z} - B_{1z} - B_{4z}) / 2d \\ \partial B_z / \partial z = -(\partial B_x / \partial x + \partial B_y / \partial y) \end{cases} \quad (8)$$

where B_{ij} is the target response. $i = 1, 2, 4, 5$ is the coils number. $j = x, y, z$ corresponds to the three components of each sensor.

In Figure 3(b), receiving coil R5 collects response data B_S . The five independent elements of matrix G are expressed as

follows:

$$\begin{cases} \partial B_x / \partial x = (B_{7x} + B_{8x} + B_{9x} - B_{1x} - B_{2x} - B_{3x}) / 6d \\ \partial B_x / \partial y = (B_{7y} + B_{8y} + B_{9y} - B_{1y} - B_{2y} - B_{3y}) / 6d \\ \partial B_x / \partial z = (B_{7z} + B_{8z} + B_{9z} - B_{1z} - B_{2z} - B_{3z}) / 6d \\ \partial B_y / \partial y = (B_{3y} + B_{6y} + B_{9y} - B_{1y} - B_{4y} - B_{7y}) / 6d, \\ \partial B_y / \partial z = (B_{3z} + B_{6z} + B_{9z} - B_{1z} - B_{4z} - B_{7z}) / 6d \\ \partial B_z / \partial z = -(\partial B_x / \partial x + \partial B_y / \partial y) \end{cases} \quad (9)$$

where B_{ij} is the target response. $i = 1, 2, 3, 4, 6, 7, 8, 9$ is the number of the eight sensors. $j = x, y, z$ corresponds to the three components of each sensor. All receiving coils are utilized to improve the localization accuracy.

According to the magnetic gradient tensor constructed in Figure 3(a), the shallow target can be located using Equation (5) to Equation (8). In Figure 3(b), the deep target can be located by Equations (5, 6, and 9).

B. TARGET LOCALIZATION PROCESS

Figure 4 is the target response collection and localization. The target localization process is based on the towed TEM sensor array. First, the target response is obtained by nine receiving coils. The early and late responses are drawn. Second, according to the maximum responses, the number and horizontal position of underground targets are roughly determined, and the magnetic gradient is constructed to further locate underground targets.

On the basis of the above-mentioned sensor array and magnetic gradient tensor localization theory, the effectiveness of the proposed method is verified by field experiments. The experiments and the analysis are discussed in the next section.

IV. EXPERIMENT DESIGN AND DISCUSSION

On the basis of the towed TEM system, the field experiment was carried out in the southern suburb of Changchun City, Jilin Province. The experiments are described in detail below.

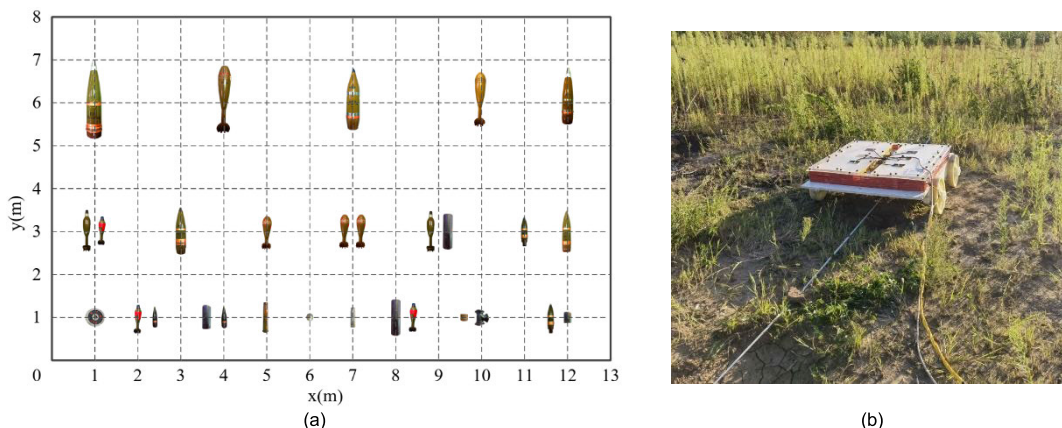


FIGURE 6. (a) Diagram of the targets distribution, (b) diagram of the towed array system.

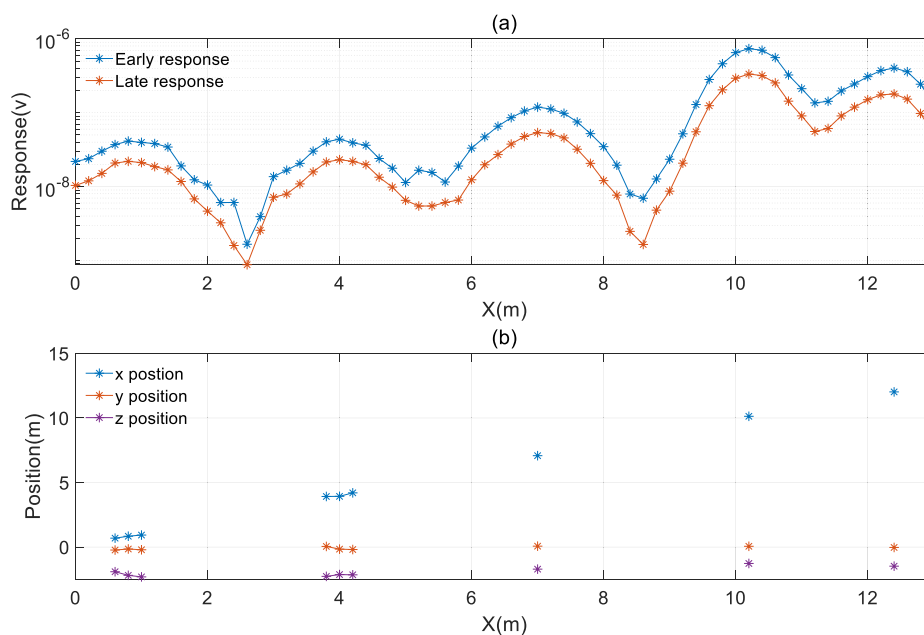


FIGURE 7. Survey line at $y = 6$ m: (a) target response, (b) target localization.

A. EXPERIMENT DESIGN

In the field experiment, 12 UXOs and 9 harmless targets were buried. The diagram and detailed parameters of the targets are shown in Figure 5 and Table 2, respectively.

As shown in Figure 5, the UXOs are numbered from U1 to U12, and the harmless targets are numbered from O1 to O9. In Table 2, the length of the UXOs ranges from 18 cm to 65 cm, and the diameter ranges from 37 mm to 130 mm. A total of 19 UXOs were buried. The lengths of the two cartridge cases (O1, O2) are 16 and 25 cm, with diameters of 30 and 37 mm, respectively. O3 to O6 are iron pipes, with a diameter of 75 mm and lengths ranging from 5 cm to 30 cm. O7 is a discus with a length and a diameter of 2 cm and 150 mm, respectively. O8 is an iron ball with a diameter of

64 mm. O9 is a three-way tube with a height of 12.5 cm. A total of 10 harmless targets were buried.

The experimental site has an area of $13\text{ m} \times 8\text{ m}$. Twenty-nine targets were buried, and the specific target distribution is shown in Figure 6. A total of 19 UXOs and 10 harmless targets were buried in the area. At survey line $y = 1$ m, five groups of multiple targets and four single harmless targets were buried at the approximate depth of 0.5 m. At $y = 3$ m, three groups of multiple targets and four single UXOs were buried at the approximate depth of 1.0 m. At $y = 6$ m, five UXOs were buried separately at different depths from 1.2 m to approximately 2.0 m. Two targets in each group are 40 cm apart. Figure 6(b) is the physical diagram of the towed TEM system.

TABLE 3. Results of target localization at y = 6 m.

Name	True position (m)	Inverted position (m)	Error (cm)
U12	(0.90, 0.00, -2.09)	(0.84, -0.15, -2.19)	(-6, -15, -10)
U11	(4.00, 0.00, -2.06)	(3.93, -0.16, -2.13)	(-7, -16, -7)
U10	(7.03, 0.00, -1.66)	(7.08, 0.07, -1.71)	(5, 7, -5)
U9	(10.09, 0.00, -1.26)	(10.13, 0.06, -1.27)	(4, 6, -1)
U8	(12.05, 0.00, -1.45)	(12.02, -0.03, -1.48)	(-3, -3, -3)

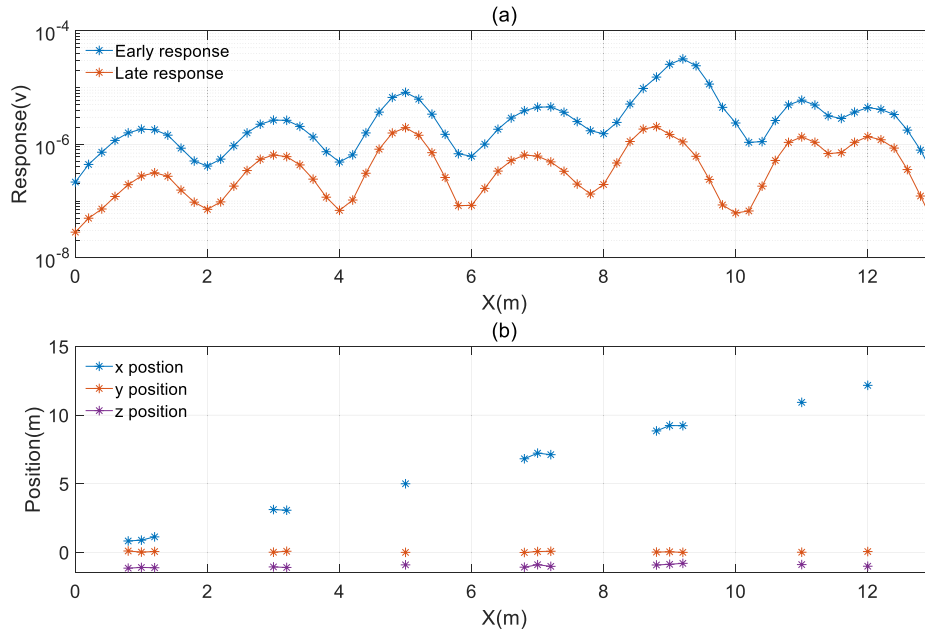


FIGURE 8. Survey line at y = 3 m: (a) target response, (b) target localization.

B. RESULTS AND DISCUSSION

In the experiment, the towed system transmitted a 12.5-Hz bipolar rectangular current with the z-component transmitting coil. Three survey lines (y = 6, 3, 1 m) were collected in the area. Sixty-six measuring points were collected in each line, and the interval between the measuring points on the survey line is 0.2 m.

The early response was calculated by averaging the responses from 0.15 ms to 0.63 ms. The late response was calculated by obtaining the average value of the responses from 2.5 ms to 15.8 ms. The results are as shown in Figure 7.

Figure 7(a) shows five groups of maxima, and are located at x = (0.8 m, 0.8 m), (4.0 m, 4.0 m), (7.0 m, 7.0 m), (10.2 m, 10.2 m), (12.4 m, 12.4 m). The maxima of the early response are approximately twice that of the late response. The horizontal positions of the maxima of the early and late responses are consistent at x = 0.8, 4.0, 7.0, 10.2, 12.4.

The early and late responses at x = 0.8, 4.0 m are weak, and the peak is relatively flat. When the system moved in the x direction from above the peak, at x = 10.2, 12.4 m, the responses slowly decayed due to the influence of the adjacent target responses. When the system moved in the x direction from above the peak x = 0.8 m, the response fluctuated and

quickly decayed due to the low SNR. From these positions, five targets at y = 6 m can be preliminarily judged.

Figure 7(b) shows five groups of target localization results. Target localization results are achieved by the average responses between 0.25 ms to 6.0 ms. The magnetic gradient tensor constructed in Figure 3(b) was used to locate underground targets according to the maximum responses. The maximum responses of the three groups at x = 7.0, 10.2, 12.4 m are obvious and have a high SNR. The horizontal positions of the maxima at the early and late responses have no difference. Therefore, the target position is estimated by a single measuring point. The maxima of the early and late responses are slightly different and weak for the remaining two groups of targets. The maximum response measuring point and two adjacent measuring points are used for localization to improve the accuracy. The results show that the localization results of the maxima responses are relatively near the true position and relatively stable. The detailed localization of the targets is shown in Table 3.

In Table 3, the depth and horizontal errors of UXO at approximately 2 m do not exceed 10 and 16 cm, respectively. The depth and horizontal errors of the target at different depths from 1.2 m to 1.6 m do not exceed 5 cm and 7 cm,

TABLE 4. Results of target localization at y = 3 m.

Name	True position (m)	Inverted position (m)	Error (cm)
U5	(0.84, 0.00, -1.03)	(0.89, 0.02, -1.10)	(5, 2, -7)
U3	(1.19, 0.00, -1.04)	(1.13, 0.06, -1.12)	(-6, 6, -8)
U7	(3.06, 0.00, -1.02)	(3.12, 0.01, -1.06)	(6, 1, -4)
U4	(5.02, 0.00, -0.85)	(5.00, 0.00, -0.91)	(-2, 0, -6)
U4	(6.85, 0.00, -1.06)	(6.82, -0.01, -1.08)	(-3, -1, -2)
U4	(7.29, 0.00, -0.80)	(7.23, 0.06, -0.90)	(-6, 6, -10)
U5	(8.77, 0.00, -0.86)	(8.85, 0.02, -0.92)	(8, 2, -6)
O6	(9.24, 0.00, -0.72)	(9.23, 0.00, -0.80)	(-1, 0, -8)
U2	(11.00, 0.00, -0.82)	(10.93, 0.01, -0.89)	(-7, 1, -7)
U6	(12.10, 0.00, -0.98)	(12.17, 0.06, -1.01)	(7, 6, -3)

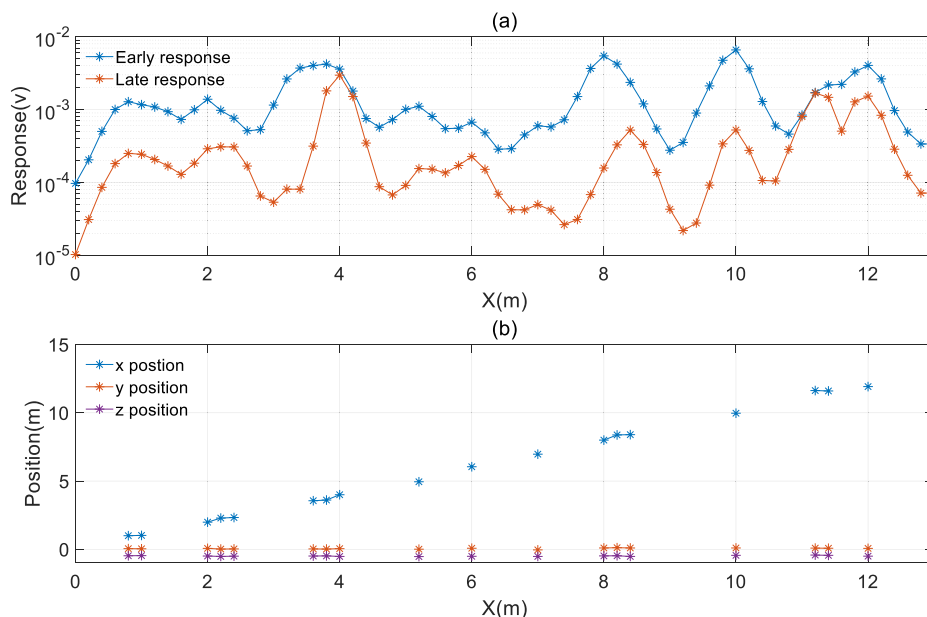


FIGURE 9. Survey line at y = 3 m: (a) target response, (b) target localization.

respectively. The result shows that the depth errors of the target do not exceed 10 cm, and the magnetic gradient tensor constructed in Figure 3(b) can accurately locate single underground targets within 2 m.

According to the obtained responses with y = 3.0 m and the magnetic gradient tensor constructed in Figure 3(b), the results are shown in Figure 8.

Figure 8(a) shows seven groups of maxima. The maxima of the early and late responses are located at x = (1.0 m, 1.2 m), (3.0 m, 3.0 m), (5.0 m, 5.0 m), (7.2 m, 6.8 m), (9.2 m, 8.8 m), (11.0 m, 11.0 m), (12.0 m, 12.0 m). The early and late response peaks of x = (1.0 m, 1.2 m), (7.2 m, 6.8 m), (9.2 m, 8.8 m) are inconsistent, indicating six targets. The horizontal positions of the remaining four groups of maximum responses are consistent, indicating four targets. The results show 10 targets at y = 3 m. Figure 8(b) shows the localization results. The maxima of the early and late responses at x = 5.0, 11.0, 12.0 m have a high SNR. Therefore, the three groups of targets can be located by a single point. The horizontal positions of the early and late responses maxima are slightly different for the remaining four groups of targets. Thus, the

maximum response and adjacent measuring points are used to estimate the target position, and the localization of the maxima responses are near the true positions. Figure 8(b) shows that the target position can be accurately estimated by the magnetic gradient.

According to the magnetic gradient tensor constructed in Figure 3(b), the target localization at y = 3.0 m is shown in Table 4. In Table 4, the horizontal and depth errors of the buried single target do not exceed 7 cm. The horizontal and depth errors of the multi-target do not exceed 8 and 10 cm, respectively. The localization results show that the magnetic gradient tensor constructed in Figure 3(b) can effectively reduce the localization errors caused by the overlapping responses of adjacent targets and accurately locate the target within 1 m.

According to the obtained responses at y = 1.0 m and the magnetic gradient tensor constructed in Figure 3(a), the results are shown in Figure 9.

Figure 9(a) shows 10 groups of maxima of the early and late responses at x = (0.8 m, 0.8 m), (2.0 m, 2.2 m), (3.8 m, 4.0 m), (5.2 m, 5.2 m), (6.0 m, 6.0 m), (7.0 m, 7.0),

TABLE 5. Results of target localization at $y = 1$ m.

Name	True position (m)	Inverted position (m)	Error (cm)
O7	(1.00, 0.00, -0.46)	(1.02, 0.04, -0.46)	(2, 4, 0)
U3	(2.00, 0.00, -0.45)	(1.99, 0.07, -0.49)	(-1, 7, -4)
U1	(2.40, 0.00, -0.46)	(2.33, 0.03, -0.50)	(-7, 3, -4)
O5	(3.60, 0.00, -0.45)	(3.61, 0.02, -0.48)	(1, 2, -3)
U1	(4.00, 0.00, -0.49)	(4.00, 0.05, -0.52)	(0, 5, -3)
O2	(5.00, 0.00, -0.50)	(4.95, 0.01, -0.53)	(-5, 1, -3)
O8	(6.00, 0.00, -0.47)	(6.05, 0.08, -0.51)	(5, 8, -4)
O1	(6.98, 0.00, -0.46)	(6.97, -0.04, -0.52)	(-1, -4, -6)
O6	(8.00, 0.00, -0.46)	(8.00, 0.10, -0.48)	(0, 10, -2)
U3	(8.40, 0.00, -0.47)	(8.40, 0.10, -0.52)	(0, 10, -5)
O3	(9.60, 0.00, -0.46)	/	/
O9	(10.00, 0.00, -0.43)	(9.97, 0.10, -0.44)	(-3, 10, -1)
U2	(11.60, 0.00, -0.42)	(11.63, 0.09, -0.42)	(3, 9, 0)
O4	(12.00, 0.00, -0.45)	(11.92, 0.07, -0.50)	(-8, 7, -5)

(8.0 m, 8.4 m), (10.0 m, 10.0 m), (/, 11.2 m), (12.0 m, 12.0 m). According to the maxima of the early and late responses, the early and late responses have 9 and 10 maxima, respectively. The response peaks of $x = (2.0$ m, 2.2 m), (3.8 m, 4.0 m), (8.0 m, 8.4 m), (/, 11.2 m) are inconsistent, indicating seven targets. The horizontal positions of the remaining six groups of maximum responses are consistent, indicating six targets. The results show 13 targets at $y = 1$ m.

Figure 9(b) shows 10 groups of localization results. The five positions at $x = 5.2, 6.0, 7.0, 10.0, 12.0$ m estimate the target position using a single point. Differences exist in the horizontal positions of the maxima of the early and late responses in the remaining five positions. Thus, the maximum response and adjacent measuring points are used to estimate the target position, and the localization of the maxima responses are relatively near the true position.

According to the maxima responses and the magnetic gradient constructed in Figure 3(a), the target localization results are shown in Table 5.

As shown in Table 5, the true depths of the targets are approximately 40 cm to 50 cm. The horizontal and depth errors of a single target do not exceed 8 and 6 cm, respectively. The horizontal and depth errors of multi-targets do not exceed 10 and 5 cm, respectively. The response of target O3 at $x = 9.6$ m is extremely weak, and the localization failed due to the response of the adjacent targets. The results show that the magnetic gradient tensor constructed in Figure 3(a) can accurately locate the target at the depth of approximately 0.5 m.

In general, according to the maxima of the early and late responses, the magnetic gradient tensor constructed in this study can effectively and accurately locate underground targets within a 2-m depth.

V. CONCLUSION

On the basis of the responses collected by a towed TEM system with a 3×3 sensor array, the two kinds of magnetic gradient tensors constructed in this study can accurately locate targets within 2 m.

The towed system consists of three transmitting coils and nine receiving coils. The z-component transmitting coil

transmits a rectangular current of 12.5 Hz, and the 3×3 sensor array obtains the target response to estimate the target position.

The combination of the magnetic gradient tensor with the early and late responses can effectively distinguish the number of targets and considerably reduce the localization error caused by the overlapping responses of adjacent targets. According to the maxima of the early and late responses, the two forms of magnetic gradient tensors constructed using four sensors can effectively reduce the magnetic gradient error for shallow targets. The magnetic gradient tensor constructed using nine sensors can accurately detect deep targets and improve the SNR. The experimental results show that the proposed method can locate underground targets within 2 m, and the depth error does not exceed 10 cm.

In summary, the proposed method can effectively locate underground targets within 2 m and provide a research method for transient electromagnetic fast detection and the identification of targets.

REFERENCES

- [1] O. O. Bilukha, M. Brennan, and M. Anderson, "Injuries and deaths from landmines and unexploded ordnance in Afghanistan, 2002-2006," *J. Amer. Med. Assoc.*, vol. 298, no. 5, pp. 516-518, Aug. 2007.
- [2] P. B. Weichman, "Validation of advanced EM models for UXO discrimination," *IEEE Trans. Geosci. Remote Sens.*, vol. 51, no. 7, pp. 3954-3967, Jul. 2013.
- [3] R. Bowers and B. Bidwell, "Geophysics and UXO detection," *Lead. Edge*, vol. 18, no. 12, pp. 1389-1391, 1999.
- [4] P. Bestagini, F. Lombardi, M. Lualdi, F. Picetti, and S. Tubaro, "Landmine detection using autoencoders on multipolarization GPR volumetric data," *IEEE Trans. Geosci. Remote Sens.*, vol. 59, no. 1, pp. 182-195, Jan. 2021.
- [5] Y. Sun and J. Li, "Time-frequency analysis for plastic landmine detection via forward-looking ground penetrating radar," *IEE Proc., Radar, Sonar Navigat.*, vol. 150, no. 4, pp. 253-261, 2003.
- [6] M. Wigh, T. Hansen, and A. Dössing, "Inference of unexploded ordnance (UXO) by probabilistic inversion of magnetic data," *Geophys. J. Int.*, vol. 1, no. 1, pp. 37-58, 2020.
- [7] J. Liu, X. Li, and X. Zeng, "A real-time magnetic dipole localization method based on cube magnetometer array," *IEEE Trans. Magn.*, vol. 55, no. 8, Aug. 2019, Art. no. 4003609.
- [8] L. Wang, S. Zhang, S. Chen, and H. Jiang, "Fast localization of underground targets by magnetic gradient tensor and Gaussian-Newton algorithm with a portable transient electromagnetic system," *IEEE Access*, vol. 9, pp. 148469-148478, 2021.
- [9] L.-P. Song, D. Oldenburg, L. R. Pasion, S. D. Billings, and L. Beran, "Temporal orthogonal projection inversion for EMI sensing of UXO," *IEEE Trans. Geosci. Remote Sens.*, vol. 53, no. 2, pp. 1061-1072, Feb. 2015.

- [10] J. P. Fernandez, B. E. Barrowes, T. M. Grzegorzczak, N. Lhomme, K. O'Neill, and F. Shubitidze, "A man-portable vector sensor for identification of unexploded ordnance," *IEEE Sensors J.*, vol. 11, no. 10, pp. 2542–2555, Oct. 2011.
- [11] J. P. Fernández, "MPV-II: An enhanced vector man-portable EMI sensor for UXO identification," *Proc. SPIE-The Int. Soc. Opt. Eng.*, vol. 8017, no. 1, 2011, Art. no. 801707.
- [12] S. Chen, S. Zhang, H. Jiang, and J. Zhu, "Location and characterization of unexploded ordnance-like targets with a portable transient electromagnetic system," *IEEE Access*, vol. 8, pp. 150174–150185, 2020.
- [13] M. Prouty, D. C. George, and D. D. Snyder, "MetalMapper: A multi-sensor TEM system for UXO detection and classification," ESTCP, Boston, MA, USA, Tech. Rep. MR-200603, Feb. 2011.
- [14] E. Gasperikova, J. T. Smith, H. F. Morrison, and A. Becker, "Berkeley UXO discriminator (BUD)," U.S. Dept. Defense, Washington, DC, USA, Tech. Rep. ProjectUX-0437, 2007.
- [15] D. Steinhurst, G. Harbaugh, J. Kingdon, and T. Furuya, "EMI array for cued UXO discrimination," *Seg Expanded Abstr.*, vol. 27, no. 1, p. 2907, 2008.
- [16] H. Jin, J. Guo, H. Wang, Z. Zhuang, J. Qin, and T. Wang, "Magnetic anomaly detection and localization using orthogonal basis of magnetic tensor contraction," *IEEE Trans. Geosci. Remote Sens.*, vol. 58, no. 8, pp. 5944–5954, Aug. 2020.
- [17] F. Shubitidze, J. P. Fernandez, B. E. Barrowes, I. Shamatava, A. Bijamov, K. O'Neill, and D. Karkashadze, "The orthonormalized volume magnetic source model for discrimination of unexploded ordnance," *IEEE Trans. Geosci. Remote Sens.*, vol. 52, no. 8, pp. 4658–4670, Aug. 2014.
- [18] T. Nara, S. Suzuki, and S. Ando, "A closed-form formula for magnetic dipole localization by measurement of its magnetic field and spatial gradients," *IEEE Trans. Magn.*, vol. 42, no. 10, pp. 3291–3293, Oct. 2006.



SHUANG ZHANG received the Ph.D. degree in circuits and systems from Jilin University, Jilin, China, in 2008. He has developed land and marine proton precession magnetic sensor based on pre-polarization and dynamic nuclear polarization effect for weak magnetic detection, detecting landmines and unexploded ordnance. He is currently a Professor with the College of Electronic Science and Engineering, Jilin University. His current research interests include weak signal detection, electromagnetic detection theory, and system design.



SHUDONG CHEN received the Ph.D. degree in instrument science and technology from Jilin University, Jilin, China, in 2012. He has developed portable and vehicle transient electromagnetic systems for detecting landmines and unexploded ordnance. He is currently an Associate Professor with the College of Electronic Science and Engineering, Jilin University. His current research interests include weak signal detection, electromagnetic detection theory, and system design.



LIJIE WANG received the B.S. degree in electronic information engineering from the Tianjin University of Science and Technology, Tianjin, China, in 2016, and the M.S. degree in electronic communication engineering from the Changchun University of Science and Technology, Jilin, China, in 2019. She is currently pursuing the Ph.D. degree in circuits and systems with Jilin University, Jilin. Her research interests include electromagnetic detection theory and data processing.

CHAOPENG LUO is currently an Engineer with the Science and Technology on Near Surface Detection Laboratory, Wuxi, China. His current research interest includes near surface detection technology.

• • •